Correction Technique for On-Chip Modulation Response Measurements of Optoelectronic Devices

Peter Debie and Luc Martens, *Member, IEEE*

***Abstract*—A new and accurate error correction technique for on-chip intensity modulation response measurements of high-frequency optoelectronic devices is presented. Mathematical expressions for the different sources of errors that exist in the measurement system are derived. The new correction technique applied to the modulation response measurement of a strained quantum well laser diode shows excellent agreement with the theoretically expected result. Simulation results for a small-signal circuit model of the laser diode show excellent agreement with the measured input reflection coefficient (S_{11} and the modulation response S_{21}. With the corrected modulation response measurement, more accurate parameters for this model are extracted.**

I. Introduction

FOR the design and development of high-speed/high-frequency optoelectronic systems, efficient and accurate models of optoelectronic devices such as laser diodes, photodiodes, and light-emitting diodes are required. These models have to be implemented in conventional electrical microwave circuit simulators like SPICE, Microwave Design System (MDS), or Touchstone, so the electrical and optical behavior of the optoelectronic device can be analyzed in the same environment. If we are also able to implement models for optical components, like for instance, optical fibers, optical modulators, optical amplifiers, and attenuators, we can even analyze complete lightwave/microwave systems with this conventional electrical microwave simulator [1]. Several types of models for optoelectronic devices have already been described [2]–[10]. Up to now it has been neglected that the accuracy of these models is dependent on the accuracy of the measured device characteristics and the extracted model parameters, although this is common knowledge for the modeling of electronic devices [11], [12].

A first step in the development of the models is the measurement of the characteristics of the optoelectronic device, such as PI (light-current) characteristics, VI (voltage-current) characteristics, high-frequency reflection coefficient, high-frequency intensity modulation characteristic, and high-speed step response. It is obvious that the accuracy of optoelectronic device circuit models strongly depends upon the accuracy of these measured characteristics. It is therefore desirable to perform the device measurements with as little parasitic influences as possible, so measurements that can be performed directly on the unpackaged device (on-chip) have a great advantage where the measurement accuracy is considered. A second, and equally important step, is the development of extraction algorithms to determine the necessary model parameters with sufficient accuracy out of this device characterization. Again, the imperfection of these algorithms impose an error on the extracted model parameters.

In this paper we present an accurate error correction technique for the on-chip modulation response measurement of high-frequency optoelectronic devices. This method takes more errors into account in order to improve the accuracy of previously reported methods [13]–[15]. We will start with a theoretical discussion of the different errors that exist in the measurement setup, and we derive mathematical expressions for them. We also present experimental results for a strained quantum well laser diode, although the same concept is also valid for other optoelectronic devices. These results show better correspondence between the measured modulation response and the theoretically expected result. Out of the corrected modulation response measurement and the measured input reflection coefficient (S_{11}), we extract parameters for a small-signal circuit model of the laser. These parameters are compared with the parameters extracted from the modulation response measurement corrected with the conventional response calibration.

II. Measurement Setup

The measurement system that we use is depicted in Fig. 1 for the case of a laser diode as device under test. It consists of a conventional vector network analyzer (HP8510C) that is extended with a lightwave test set (HP83420A) [15]. This means that this analyzer system has two electrical and two optical ports, so it allows us to characterize electrical devices as well as optical and optoelectronic two-port devices. In the lightwave test set, a calibrated laser diode and photodiode are used for the electrical-optical and optical-electrical conversions. To measure the modulation response of a laser diode, respectively photodiode, the measured response of the combined laser diode/photodiode system is divided by the response data of the calibrated photodetector, respectively calibrated laser diode. In this way, the magnitude and the phase can be measured, so the system in Fig. 1 has vector network analyzer capabilities for electrical, as well as for optoelectronic and optical devices. Contact with the coplanar electrical port of the optoelectronic device is established with a ground-signal-ground (GSG) microwave wafer probe.

Manuscript received June 13, 1994; revised September 27, 1994.

The authors are with the Department of Information Technology, University of Gent—IMEC, 9000 Gent, Belgium.

IEEE Log Number 9410710.

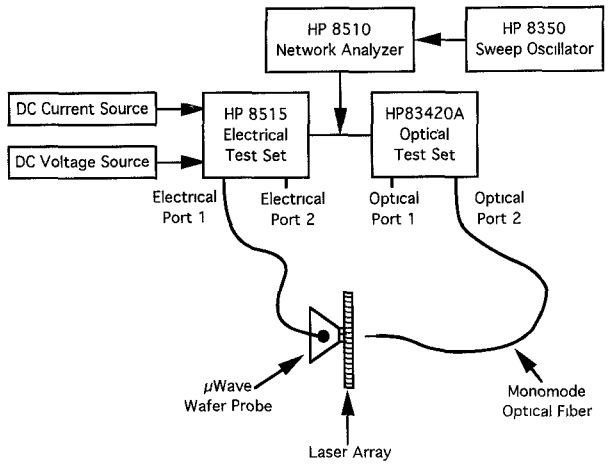

Fig. 1. Schematic of the lightwave component analyzer system.

Due to the nature of the optoelectronic devices, the lightwave test set supports only a simple response calibration. This means that the microwave probe cannot be included in the calibration because a thru connection between the coplanar tip of the wafer probe and the coaxial output of the photodetector cannot be realized. The response calibration provides only a signal path frequency response error correction. This may be adequate for measurements of well matched, low loss devices, but this is normally not the case for optoelectronic devices. We use, therefore, an error model that is based on a conventional 12-term error model [16], [17] for the correction of electrical two-port measurements.

III. Error Correction Model

The flow graph of the conventional response error model, in the case of a laser diode as device under test, is presented in Fig. 2. The reference planes after this response calibration are located before the coplanar probe and behind the photodetector. Also, input and output errors are neglected or simplified in this model. This means that the mismatch between the microwave probe, network analyzer source, laser diode, photodiode, and network analyzer receiver is neglected. Optoelectronic devices, however, are usually not well matched, so this can give significant measurement errors. E_{TFr} and E_{RFr} are the correction coefficients for the signal path frequency response error.

The flow graph of the new error correction model we developed is presented in Fig. 3. This model provides directivity (E_{DF}), isolation (E_{XF}), source match (E_{SF}), load match (E_{LF}), and frequency response (E_{TF} and E_{RF}) error correction. The isolation term is usually very small and will not be included further in this discussion. Due to the nature of the devices, the S_{12}^{l+p} coefficient of the combined laser diode/photodiode system can be neglected. This means that we do not take into account optical effects, like for instance, the optical reflections on the calibrated photodetector and laser diode under test. For the type of devices that we consider here, these effects are extremely low, and therefore negligible. This implies that the modulation response of the combined laser diode/photodiode system (S_{21}^{l+p}) is defined as the product of the individual responses of the laser diode and photodiode

$$S_{21}^{l+p} = S_{21}^{\mathrm{laser}} \cdot S_{21}^{\mathrm{photodiode}}. \tag{1}$$

The reference planes in Fig. 3 are located just before the laser input and just after the photodiode. By comparing the two error models of Figs. 2 and 3, it is easy to see that the conventional response error correction does not take into account the following five errors: attenuation of the microwave wafer probe, mismatch of laser input and probe output, mismatch of probe input and source output, mismatch of photodetector output and receiver input, and the error on the transmission coefficient of the response calibration. This means that the laser modulation response measured with the conventional response calibration ($S_{21}^{\mathrm{response}}$) has to be corrected in order to obtain a more accurate modulation response measurement (S_{21}^{laser})

$$S_{21}^{\mathrm{laser}} = \Gamma \cdot S_{21}^{\mathrm{response}}. \tag{2}$$

Γ is a correction factor given by

$$\Gamma = \gamma_p \cdot \gamma_{l+p} \cdot \gamma_{p+s} \cdot \gamma_{ph+rx} \cdot \gamma_r. \tag{3}$$

From the error model of Fig. 3, straightforward calculations result in the following expressions for the different error correction coefficients:

$$\gamma_p = \frac{1}{S_{21}^{\mathrm{probe}}} \tag{4}$$

for the probe attenuation

$$\gamma_{l+p} = 1 - S_{22}^{\mathrm{probe}} \cdot S_{11}^{\mathrm{laser}} \tag{5}$$

for the laser input and probe output mismatch

$$\gamma_{p+s} = 1 - E_{\mathrm{SF}} \cdot \frac{S_{11}^{\mathrm{probe}} - S_{11}^{\mathrm{laser}} \cdot \det[S^{\mathrm{probe}}]}{1 - S_{22}^{\mathrm{probe}} \cdot S_{11}^{\mathrm{laser}}} \tag{6}$$

for the probe input and the source output mismatch

$$\gamma_{ph+rx} = 1 - S_{22}^{\mathrm{photodiode}} \cdot E_{\mathrm{LF}} \tag{7}$$

for the photodiode output and receiver input mismatch, and

$$\gamma_r = \frac{1}{1 - E_{\mathrm{SF}} \cdot E_{\mathrm{LF}}} \tag{8}$$

for the transmission coefficient of the response calibration.

The error coefficients in (7) and (8) are second order effects because the photodiode output, receiver input, and source output are well matched. The contribution of these two factors is much smaller than the other error correction factors, and therefore, they are not further included in this discussion. Measurement results also showed that these two error coefficients were negligible compared to the other three errors. In order to calculate the error coefficients (4)–(6), the scattering parameters of the microwave probe (S_{11}^{probe}, S_{22}^{probe} and $S_{12}^{\mathrm{probe}} \cdot S_{21}^{\mathrm{probe}}$), the reflection coefficient of the laser (S_{11}^{l+p}), and the reflection coefficient of the network analyzer source (E_{SF}) are needed. The reflection coefficient of the source has been measured with a conventional coaxial full one-port calibration. The input reflection of the laser has been

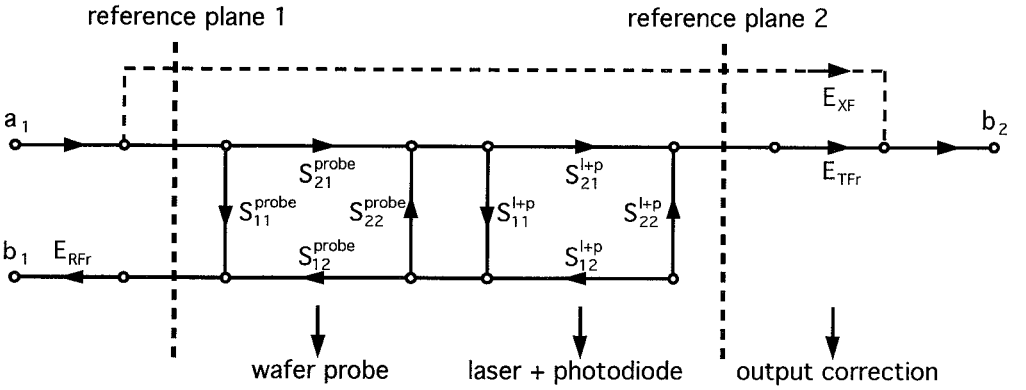

Fig. 2. Conventional response calibration error model.

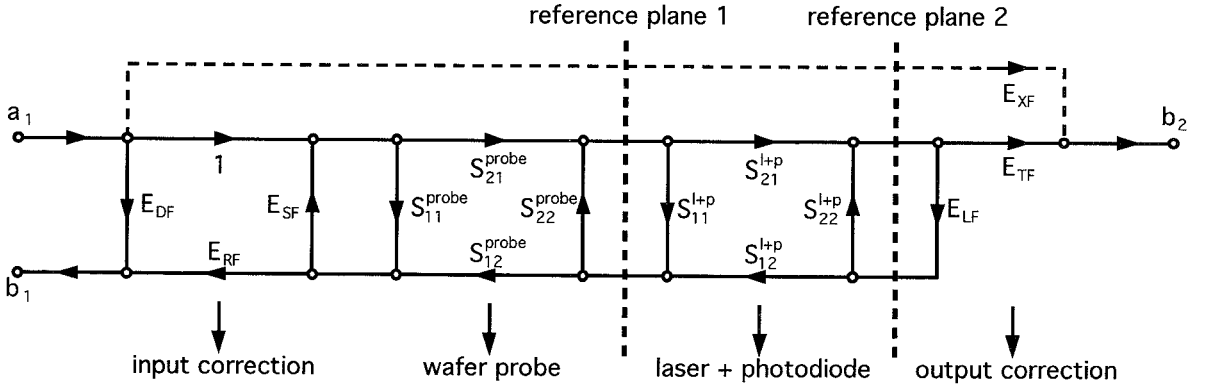

Fig. 3. Flow graph of the presented error correction model.

measured with a full one-port on-wafer calibration at the probe tip.

For the determination of the S-parameters of the microwave probe, first a full one-port calibration was performed at the coaxial input of the probe. Afterwards, three known impedance standards (short, open, and load) have been measured on-wafer using this coaxial full one-port calibration. With these three calibration measurements, the probe parameters necessary for (4)–(6) have been determined [13], [14].

IV. Application of the Error Correction Technique

Strained quantum well lasers are the latest generation of semiconductor lasers. Especially strained InGaAs-AlGaAs quantum well laser diodes are well suited for the pumping of Erbium-doped fiber amplifiers because of their high output power and short wavelength (900–1100 nm). High power applications are, however, not the only field of interest for the development of strained InGaAs-AlGaAs laser diodes. Due to the low threshold current density of the InGaAs-AlGaAs quantum well material and the relatively high intensity modulation bandwidth, which already has been reported up to a maximum of 28 GHz [18], this type of laser diode becomes also well suited for applications like optical computing and short optical interconnections [19], [20]. Although quantum well lasers are based on a relatively new technology, it seems likely that they will eventually replace most of the existing laser types [10]. If we can develop models for this type of devices for use in conventional microwave circuit simulators, we can reduce the product cost and design time of such optical communication systems.

Fig. 4 shows a detailed photograph of the laser diode under test. It is a ridge waveguide InGaAs-AlGaAs strained quantum well laser with an optical wavelength of 0.98 μm. Because the p-contact of the laser is located on top of the device and the n-contact at the bottom, the laser diode is mounted on an alumina substrate. The p-contact is connected to a short coplanar line with a bond wire, so we must use a GSG microwave wafer probe to make electrical contact with the device. The right hand side of Fig. 4 shows the monomode fiber that is used to capture the laser light. The fiber is mounted on a micropositioner, so it can be moved as close as possible to the device. In this way, sufficient laser light can be captured to measure the modulation response.

Fig. 5 shows the significance of the three dominant error correction coefficients for the laser diode. It can be seen that the probe attenuation is the most drastic error, but the other two factors are not so small that they can be neglected. Fig. 5 also shows the total error correction coefficient Γ. When these errors are taken into account, the measurement uncertainty is reduced with ± 3 dB. Fig. 6 shows the final result for the modulation response of the laser diode with a bias current of 100 mA. The graph shows the characteristic with and

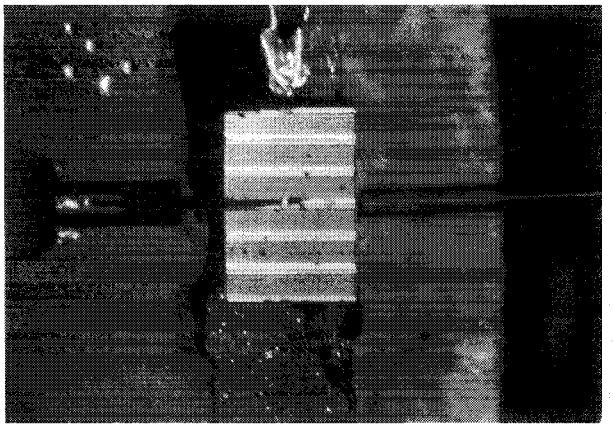

Fig. 4. Detailed photograph of the strained quantum well laser diode under test.

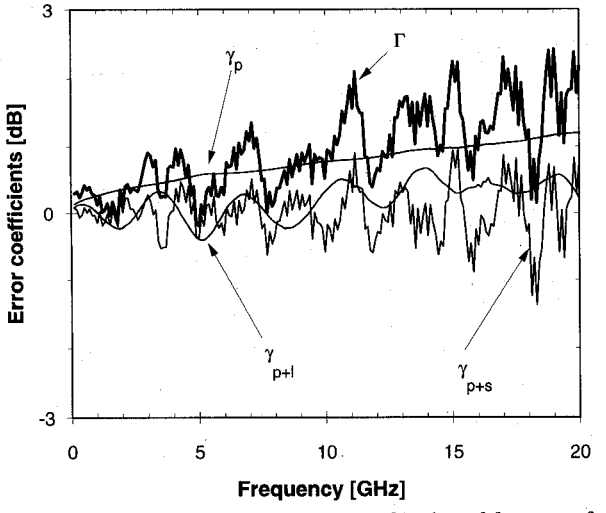

Fig. 5. Three significant error coefficients as a function of frequency for a strained quantum well laser diode.

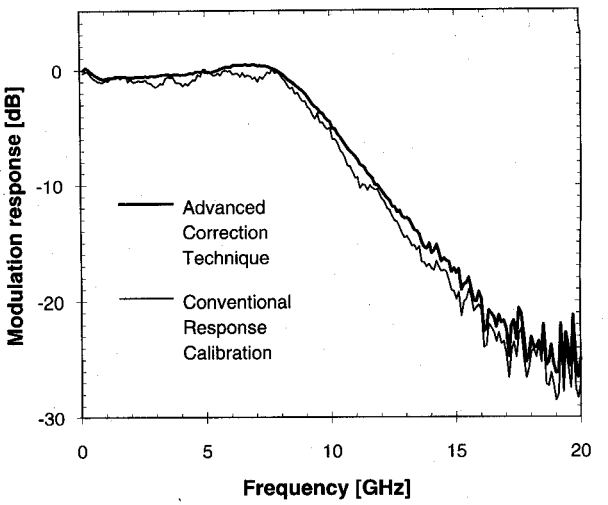

Fig. 6. Modulation response with and without the presented error correction method for a strained quantum-well laser diode ($I_{\text{bias}} = 100$ mA, $\lambda = 1$ μm).

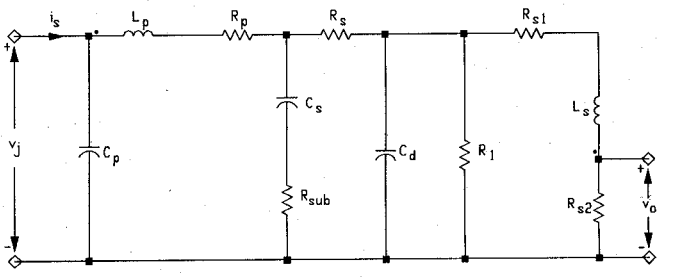

Fig. 7. Small-signal circuit model of a strained quantum-well laser diode.

without the improved error correction method. It can be clearly seen from this picture that the corrected curve shows better overall correspondence with the theoretically expected result. The measurement with the conventional response calibration shows a typical input mismatch ripple, and the resonance peak is not visible. This resonance peak can be distinguished in the corrected measurement and also the ripple has disappeared.

Making accurate measurements is very important when parameters have to be extracted for modeling the device under test. For the laser diode, several models have already been proposed [2]–[10]. A typical small-signal circuit model of the laser diode, that can be used in all conventional microwave circuit simulators, is shown in Fig. 7. In this model, i_s and v_j are the small-signal components of the input current and the junction voltage, respectively, and v_s is proportional to the small-signal light output intensity. The model includes the electrical parasitics such as the bond-wire inductance (L_p) and resistance (R_p), and a shunt capacitance (C_p) to ground. The most dominant electrical parasitics associated with the device itself are also included, such as the total series resistance (R_s), the shunt capacitance (C_s) associated with the different layers of the device, and the substrate resistance (R_{sub}). Charge storage in the active layer is modeled by the capacitance C_d, and the small-signal photon storage is modeled by the inductance L_s. The relaxation oscillation is a resonance between the capacitance C_d and the inductance L_s, representing an exchange of energy between carriers and photons, respectively. Damping of this resonance is modeled by the three resistances R_1, R_{s1}, and R_{s2}.

The values of the parasitic circuit elements can be easily obtained from microwave reflection coefficient measurements [8], [21]. The parameters of the active region were initially estimated using process parameters of the device, like the optical gain, photon lifetime, volume of the active region, etc. These parameters were adjusted to get an optimum match between the modeled and measured modulation response and between the modeled and measured reflection coefficient. The result of this approach for the strained quantum well laser diode with a bias current of 100 mA is shown in Fig. 8 for the reflection coefficient and in Fig. 9 for the modulation response. Table I lists the extracted model parameters for this device. The model parameters extracted from two modulation response measurements, one corrected with the presented technique and one corrected with the conventional technique, are compared. Some of the extracted parameter values change more than 50% when the inaccurate measurement technique is used, proving that accurate device characterization is necessary for extracting accurate optoelectronic device model parameters.

TABLE I
EXTRACTED MODEL PARAMETERS FOR A STRAINED QUANTUM-WELL LASER DIODE

Parameter	Symbols and Units	Values Extracted using the Presented Technique	Values Extracted using the Conventional Technique	Deviation [%]
Bond wire inductance	L_p (nH)	0.868	0.868	0.0
Bond wire resistance	R_p (Ω)	0.832	1.011	21 5
Shunt capacitance	C_p (fF)	60.41	60 41	0.0
Laser diode series resistance	R_s (Ω)	1.130	0 951	15.8
Laser diode shunt capacitance	C_s (pF)	11.18	18.06	61 5
Substrate resistance	R_{sub} (Ω)	1.050	0.416	60.4
Charge storage capacitance	C_d (nF)	16.64	16.70	0 4
Photon storage capacitance	L_s (fH)	22.55	21.67	3 9
Resonance damping resistor	R_1 (Ω)	0.018	0.035	94 4
Resonance damping resistor	R_{s1} (mΩ)	0.630	0.620	1.6
Resonance damping resistor	R_{s2} ($\mu\Omega$)	8 932	9.015	0.9

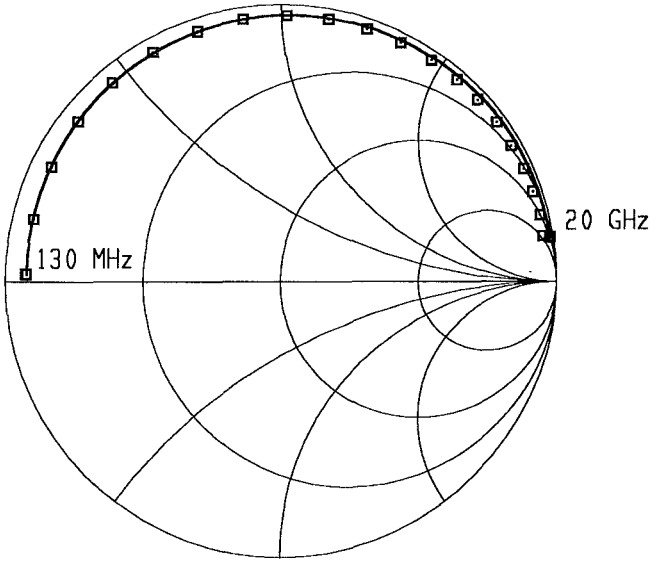

Fig. 8. Measured (□) and simulated (——) input reflection coefficient S_{11} for a strained quantum-well laser diode (I_{bias} = 100 mA).

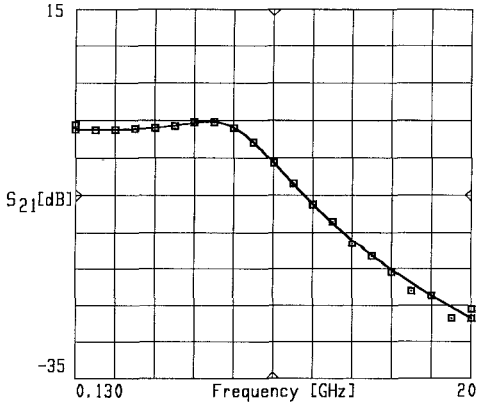

Fig. 9. Measured (□) and simulated (——) modulation response S_{21} for a strained quantum-well laser diode (I_{bias} = 100 mA).

V. CONCLUSION

A new and accurate correction technique for on-chip intensity modulation response measurements of high-frequency optoelectronic devices has been presented. Mathematical expressions for the different error sources that exist in the characterization system have been derived. Measurement results of a strained quantum well laser diode show excellent agreement between the measured modulation response and the theoretically expected result. Extraction results for a small-signal circuit model of the laser diode show that the parameter values are very sensitive to changes in the modulation response, proving that it is necessary to make accurate modulation response measurements to extract accurate model parameters for optoelectronic device circuit models. The simulated input reflection coefficient and modulation response of this model show very good agreement with measured data. The technique is very straightforward, and it can be easily implemented for future modulation response measurements.

ACKNOWLEDGMENT

The authors wish to thank G. Vermeire and F. Vermaerke for the fabrication and processing of the optoelectronic devices.

REFERENCES

[1] T Zhang, R. Hicks, and R. S. Tucker, "Computer-aided design and analysis of lightwave/microwave systems," in *IEEE Int. Microwave Symp. Dig.*, Albuquerque, NM, 1992, pp. 841–844.
[2] R. S. Tucker and I. P. Kaminow, "High-frequency characteristics of directly modulated InGaAsP ridge waveguide and buried heterostructure lasers," *J. Lightwave Technol.*, vol. LT-2, pp. 385–393, Aug. 1984.
[3] D. S. Gao *et al.*, "Modeling of quantum-well lasers for computer-aided analysis of optoelectronic integrated circuits," *IEEE J. Quantum Electron.*, vol. 26, pp. 1206–1216, July 1990.
[4] R. S. Tucker, "High-speed modulation of semiconductor lasers," *J. Lightwave Technol.*, vol. LT-3, no. 6, pp. 1180–1192, Dec. 1985.
[5] W. H. Hong *et al.*, "Circuit models for frequency modulation response of semiconductor lasers," *Electron. Lett.*, vol. 25, no. 9, pp. 591–592, Apr. 1989.
[6] C. S. Harder *et al.*, "High-speed GaAs/AlGaAs optoelectronic devices for computer applications," *IBM J. Res. Dev.*, vol. 34, no. 4, pp. 568–584, July 1990.
[7] H. Elkadi, J. P. Vilcot, and D. Decoster, "An equivalent circuit model for multielectrode lasers: Potential devices for millimeter-wave applications," *Microwave Opt. Technol. Lett.*, vol. 6, no. 4, pp. 245–249, Mar. 1993.
[8] R. S. Tucker and D. J. Pope, "Microwave circuit models of semiconductor injection lasers," *IEEE Trans. Microwave Theory Tech.*, vol. MTT-31, no. 3, pp. 289–294, Mar. 1983.

[9] E. H. Böttcher *et al.*, "Modelling and characterization of ultra high-speed InGaAs MSM photodetectors," in *Proc. 18th Euro. Conf. Opt. Commun.*, Berlin, Germany, Sept. 1992, pp. 277–280.
[10] K. Y. Lau, "Dynamics of quantum well lasers," in *Quantum Well Lasers*, P. S. Zory, Ed. New York: Academic, 1993, ch. 5 pp. 217–275.
[11] P. Debie, L. Martens, and D. De Zutter, "Fast and accurate on-wafer extraction of parasitic resistances in GaAs MESFET's," in *Proc. IEEE Int. Conf. Microelectron. Test Struct.*, San Diego, CA, Mar. 22–24, 1994, pp. 7–11.
[12] M. Golio, "Characterization, parameter extraction and modeling for high frequency applications," in *Proc. 23rd Euro. Microwave Conf.*, 1993, pp. 69–72.
[13] D. Kaiser *et al.*, "De-embedding of on-wafer lightwave measurements performed on a monolithic 10 Gb/s InP receiver-OEIC," in *Proc. 23rd Euro. Microwave Conf.*, 1993, pp. 361–363.
[14] S. H. Rumbaugh, "On-wafer photodiode measurements with a lightwave component analyzer system," presented at *Int. Optoelectron. Exh.*, Tokyo, Japan, 1991.
[15] R. W. Wong, P. Hernday, M. G. Hart, and G. A. Conrad, "High-speed lightwave component analysis," *Hewlett-Packard J.*, vol. 40, no. 3, pp. 35–51, June 1989.
[16] S. Rehnmark, "On the calibration process of automatic network analyzer systems," *IEEE Trans. Microwave Theory Tech.*, vol. MTT-22, pp. 437–438, Apr. 1974.
[17] J. Fitzpatrick, "Error models for systems measurement," *Microwave J.*, vol. 21, no. 5, pp. 63–66, May 1978.
[18] L. F. Eastman, "High speed laser diodes," in *Proc. IEEE Lasers Opt. Soc. Annu. Meet.*, 1992, pp. 23–24.
[19] F. Vermaerke *et al.*, "Simple reliable processing technique for low-threshold high-power strained InGaAs-AlGaAs GRINSCH SQW laser diodes," *IEE Proc.*, pt. J, vol. 140, no. 1, pp. 75–79, Feb. 1993.
[20] F. Vermaerke *et al.*, "Fast and reliable processing of high performance InGaAs 0.98 μm laser diodes," in *Processing Packaging Semiconductor Lasers Optoelectronic Devices*, H. Temkin, Ed., *SPIE Conf. Proc.*, Los Angeles, CA, Jan. 20–21 1993, vol. 1851, pp. 23–30.
[21] M. L. Majewski and D. Novak, "Method for characterization of intrinsic and extrinsic components of semiconductor laser diode circuit model," *IEEE Microwave and Guided Wave Lett.*, vol. 1, no. 9, pp. 246–248, Sept. 1991.

Peter Debie was born December 19, 1967, in Antwerp, Belgium. He received the degree in electrical engineering from the University of Gent, Belgium, in July 1990.

He has been a member of the research staff of the Interuniversity MicroElectronics Center (IMEC) since 1993. He is currently working towards a Ph.D. degree in electrical engineering at the Department of Information Technology (INTEC) of the University of Gent. His research focuses on all aspects of high frequency characterization and parameter extraction techniques for nonlinear circuit models of MESFET's and optoelectronic devices.

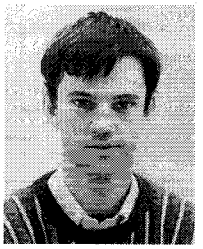

Luc Martens (M'92) was born in Gent, Belgium, on May 14, 1963. He received the degree in electrical engineering from the University of Gent in July 1986. In December 1990, he received the Ph.D. degree from the same university.

From September 1986–December 1990, he was a research assistant at the Department of Information Technology (INTEC) at the University of Gent. During this period, his scientific work was focused on the physical aspects of hyperthermic cancer therapy. His research work dealt with electromagnetic and thermal modelling and with the development of measurement systems for that application. Since January 1991, he has been a member of the permanent staff of the Interuniversity MicroElectronics Center (IMEC) and has been responsible for the research on high frequency characterization of packaging technologies and active devices at INTEC. He is also further studying topics related to the health effects of wireless communication devices. Since April 1993, he has been a professor in electrical applications of electromagnetism at the University of Gent.